Transport in Porous Media **4**: 549–565, 1989.

Numerical Simulation of Three-Dimensional Saturated Flow in Randomly Heterogeneous Porous Media

RACHID ABABOU*, DENNIS MCLAUGHLIN, LYNN W. GELHAR, and ANDREW F. B. TOMPSON
Ralph M. Parsons Laboratory, Department of Civil Engineering, Massachusetts Institute of Technology, Cambridge, MA 02139, U.S.A.

(Received: 11 April 1989)

Abstract. This paper presents a numerical method for simulating flow fields in a stochastic porous medium that satisfies locally the Darcy equation, and has each of its hydraulic parameters represented as one realization of a three-dimensional random field. These are generated by using the Turning Bands method. Our ultimate objective is to obtain statistically meaningful solutions in order to check and extend a series of approximate analytical results previously obtained by a spectral perturbation method (L. W. Gelhar and co-workers). We investigate the computational aspects of the problem in relation with stochastic concepts. The difficulty of the numerical problem arises from the random nature of the hydraulic conductivities, which implies that a very large discretized algebraic system must be solved. Indeed, a preliminary evaluation with the aid of scale analysis suggests that, in order to solve meaningful flow problems, the total number of nodes must be of the order of 10^6. This is due to the requirement that $\Delta x_i \ll \lambda_i \ll L_i$, where Δx_i is the mesh size, λ_i is a typical correlation scale of the inputs, and L_i is the size of the flow domain ($i = 1, 2, 3$). The optimum strategy for the solution of such a problem is discussed in relation with supercomputer capabilities. Briefly, the proposed discretization method is the seven-point finite differences scheme, and the proposed solution method is iterative, based on prior approximate factorization of the large coefficient matrix. Preliminary results obtained with grids on the order of one hundred thousand nodes are discussed for the case of steady saturated flow with highly variable, random conductivities.

Key words. Flow in random media, effective conductivity, finite differences, iterative methods, large-scale simulations, groundwater flow, stochastic hydrology, random functions.

1. Introduction

In this paper, we concern ourselves with the large-scale characterization of flow within naturally heterogeneous formations, including for instance the determination of the 'effective' hydraulic conductivity. The main application we have in view is the prediction of contaminant migration over large time and length scales in the vadose zone and saturated groundwaters. The solution of the saturated flow problem would constitute a first step in this direction. The naturally 'heterogeneous' porous medium is viewed here as a statistically homogeneous realization of a three-dimensional random field. Thus, the detailed spatial fluctuations of the local hydraulic properties (such as the log-conductivity)

* Now at Department of Civil Engineering and Operations Research, Princeton University, U.S.A.

are conveniently reduced to a few statistical parameters, e.g. mean, variance, and correlation lengths. Building on this, a spectral perturbation theory has been previously developed by L. W. Gelhar and co-workers, to explicitly obtain the second-order properties of the three-dimensional flow field as well as the 'effective' conductivity (Bakr *et al.*, 1978; Gelhar, 1984). In this theory, however, the mean flow solution must be known beforehand and the perturbations of the flow variables (heads, velocities) are assumed to be statistically homogeneous at all scales, or at least at some scale of interest. Furthermore, these solutions are valid only for a relatively small input variability (presumably for $\sigma_{\ln K} < 1$). It is not yet known how good these solutions are for larger standard deviations of the $\ln K$ random field.

The basic idea underlying the present work is that it is possible to obtain a statistically meaningful realization of the flow field by numerically solving the full three-dimensional flow equation, over a sufficiently large domain, for a single realization of hydraulic properties. In contrast with the infinite-domain spectral perturbation method, there is no inherent assumption concerning the statistical properties of the solution, and a finite rather than infinite length scale is implied via the size of the computational flow domain. Finally, no restriction is imposed on the magnitude of conductivity variability, apart from possible numerical constraints. We argue here that it is possible in practice to obtain reliable numerical solutions for large variabilities, say $\sigma_{\ln K} \approx 1-2$ or even more, as may be observed in some highly heterogeneous formations.

The crucial issue in the proposed approach is 'numerical feasibility'. Indeed, the domain must be discretized into a very large number of cells or nodes, of the order of one million, in order to obtain statistically significant results (large sampling domain, fine resolution). This may be feasible with current supercomputer capabilities provided that the solution method is carefully designed. Another important issue is the generation of accurate realizations of the random field of conductivity with prescribed statistics. A three-dimensional Turning Bands method was implemented for this purpose (Matheron, 1973; Mantoglou and Wilson, 1982; Tompson *et al.* 1987). The resulting realizations were used as input for the flow simulator.

The remainder of this paper focuses of the development and test of an appropriate numerical solution method for the 'random' flow problem defined above. In the next section, we emphasize some numerical requirements on the basis of scale analysis. The performance of the solution method (a preconditioned iterative solver based on finite differences) is then evaluated, along with its computational requirements. Eventually, the results obtained for typical saturated flow problems are analyzed and interpreted from a statistical viewpoint. The last section summarizes the results obtained so far, and includes a brief discussion of possible extensions of this approach to more complex flow systems (statistically anisotropic media, and unsaturated flow).

2. Scale Analysis and Numerical Requirements

In order to clarify the proposed 'single realization' approach, we define a set of length scales as follows. First, the size of the flow domain (scale of interest) is assumed to be much smaller than the regional scale, or scale of inhomogeneity $\mathscr{L}$. Consider, for instance, the variations of the log-conductivity within a region of size 10–50 km, extending from a coastal plain (sands and gravels) near the sea, to a sandstone formation towards the interior. Along a transect originating at the sea shore, the log-conductivity may vary as depicted in Figure 1. The $\ln K$ process fluctuates about a nonlinear trend $K_G(x)$; the local variance of these fluctuations decreases in the sandstone formation. One may define accordingly various scales of inhomogeneity such as

$$\mathscr{L} \approx \left(\frac{\mathrm{d} \ln K_G}{\mathrm{d}x}\right)^{-1} \quad \text{(effect of linear trend)},$$

$$\mathscr{L} \approx \left(\frac{\mathrm{d}\sigma_{\ln K}}{\mathrm{d}x}\right)^{-1} \quad \text{(effect of standard deviation trend)},$$

$$\mathscr{L} \approx \left(\frac{1}{2}\frac{\mathrm{d}^2 \ln K_G}{\mathrm{d}x^2}\right)^{-1/2} \quad \text{(effect of curvature, e.g. after linear detrending)}.$$

Typically, the size of the flow domain could be of the order $L \approx 1$–10 km (smaller than $\mathscr{L}$). The $\ln K$ process may then be assumed statistically homogeneous at the scale of the flow domain, possibly after linear detrending, as suggested in Figure 1.

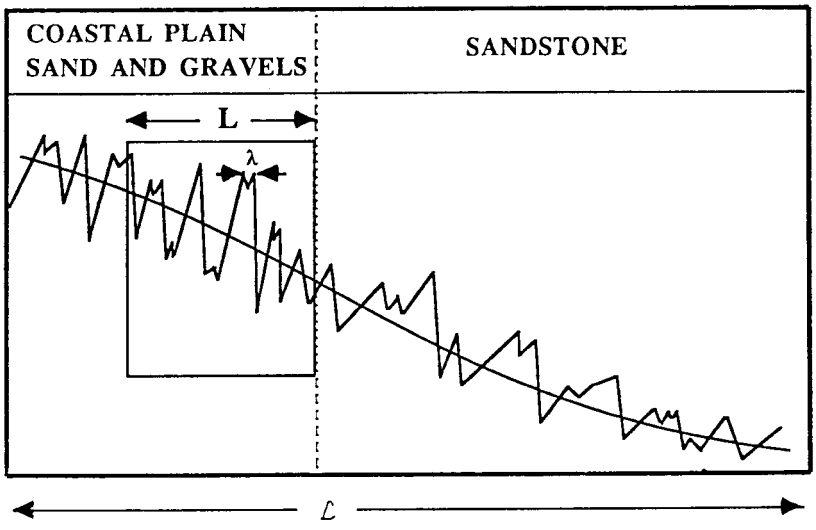

Fig. 1. Identification of scales: regional scale ($\mathscr{L}$), scale of the flow domain (L) and correlation scale (λ).

Second, we assume that the data collected at scale L will reveal the existence of a scale of fluctuation (or correlation length λ) that should be much smaller than L in order to be statistically meaningful. Thus, λ will typically be of order 10–100 m in the horizontal, and usually much less in the vertical, if the formation is stratified. This interpretation implies that the scale of fluctuation may depend on the scale of interest (L), which in turn was assumed to be smaller than some regional scale of inhomogeneity. In brief, we require

$$\lambda \ll L \ll \mathscr{L}. \tag{1}$$

Let us now examine how the size of the *numerical* problem can be related to length scales such as λ. In order to obtain a statistically meaningful realization of the hydraulic head field, the domain size should be taken much larger than the head fluctuation scale λ_H, say: $L \approx 5\lambda_H$. But from spectral perturbation results (Bakr *et al.*, 1978), we expect λ_H to be 5 to 10 times larger than $\lambda_{\ln K}$. Therefore, we need at least

$$\frac{L}{\lambda_{\ln K}} \geqslant 25. \tag{2}$$

On the other hand, the mesh size (Δx) of the discretized space must be small enough so that the statistical properties of inputs ($\ln K$) and outputs (heads, velocities) are preserved. This leads to the resolution requirement $\Delta x/\lambda_{\ln K} \ll 1$, which is similar to the sampling theorem in signal theory: a temporal signal of period T should be sampled at time intervals $\Delta t \ll T/2$ in order to avoid aliasing (in our case, the fluctuation scale λ plays the role of $T/2$). The mesh size constraint can also be interpreted as a requirement for minimizing the spatial filtering due to the discretization of the original flow equation. Heuristically, the discretization over a mesh of size Δx can be viewed as a spatial filter of bandwidth Δx. For a given ratio $\Delta x/\lambda$, the filtered input and output may be interpreted as local averages, with reduced variance and larger correlation scale compared to point processes. For a one-dimensional exponential covariance function, the statistics (σ^2, λ) will be distorted by no more than 10% upon local averaging over $\Delta x = \lambda/4$. This suggests that a reasonable resolution requirement could be

$$\frac{\Delta x}{\lambda_{\ln K}} \leqslant \frac{1}{5}. \tag{3}$$

Now, Equations (2) and (3) imply that

$$\frac{Li}{\Delta x_i} \geqslant 100, \quad i = 1, 2, 3. \tag{4}$$

Finally, due to the three-dimensionality of the problem, the total number of grid

points N in the discretized flow domain should satisfy

$$N = \left(\frac{L_i}{\Delta x_i}\right)^3 \geqslant 10^6. \tag{5}$$

The large grid size implied by (5) is due to three concurrent requirements: large sampling domain, fine resolution, and three-dimensionality. The latter feature is essential for a realistic reppresentation of the physical phenomenon. Indeed, results obtained with the spectral perturbation method proved to be very sensitive to the dimensionality of the problem. For instance, the head variance is reduced by one order of magnitude in three dimensions compared to one dimension (Bakr *et al.*, 1978).

In summary, to obtain a meaningful solution of the random flow problem by direct numerical simulation may require a grid size in the order of 1 000 000 nodes. How such large problems can be efficiently solved is now being investigated.

3. Governing Equation and Solution Methods

The saturated/unsaturated flow equation in a spatially variable medium is given most generally by

$$-S(h, \mathbf{x})\frac{\partial h}{\partial t} + \frac{\partial}{\partial x_i}\left[K(h, \mathbf{x})\left(\frac{\partial h}{\partial x_i} + g_i\right)\right] \equiv 0, \tag{6}$$

where S represents a 'storage capacity' (specific storativity or specific moisture capacity), K represents the saturated or unsaturated hydraulic conductivity, h is the water pressure head and g_i the component of a unit vector representing the acceleration of gravity (by convention $g_1 = g_2 = 0$ and $g_3 = +1$ if x_3 is vertical upwards).

In the following, we will consider the simpler problem of steady saturated flow, governed by

$$\frac{\partial}{\partial x_i}\left[K(\mathbf{x})\frac{\partial H}{\partial x_i}\right] \equiv 0, \tag{7}$$

where $H = h + g_i \cdot x_i$ is the hydraulic head. After discretization, one is left with a system of N linear algebraic equations, in the order of 1 000 000 nodes according to Equation (5).

The large size of the system to be solved has led us to search the literature for very efficient numerical solution methods which have been successfully used in subsurface hydrology and other fields (e.g. hydrodynamics and aerodynamics). The spatial discretization scheme we selected after an extensive review and some numerical tests is the seven point centered finite difference scheme. This results in the algebraic system:

$$A\mathbf{H} = \mathbf{B}, \tag{8}$$

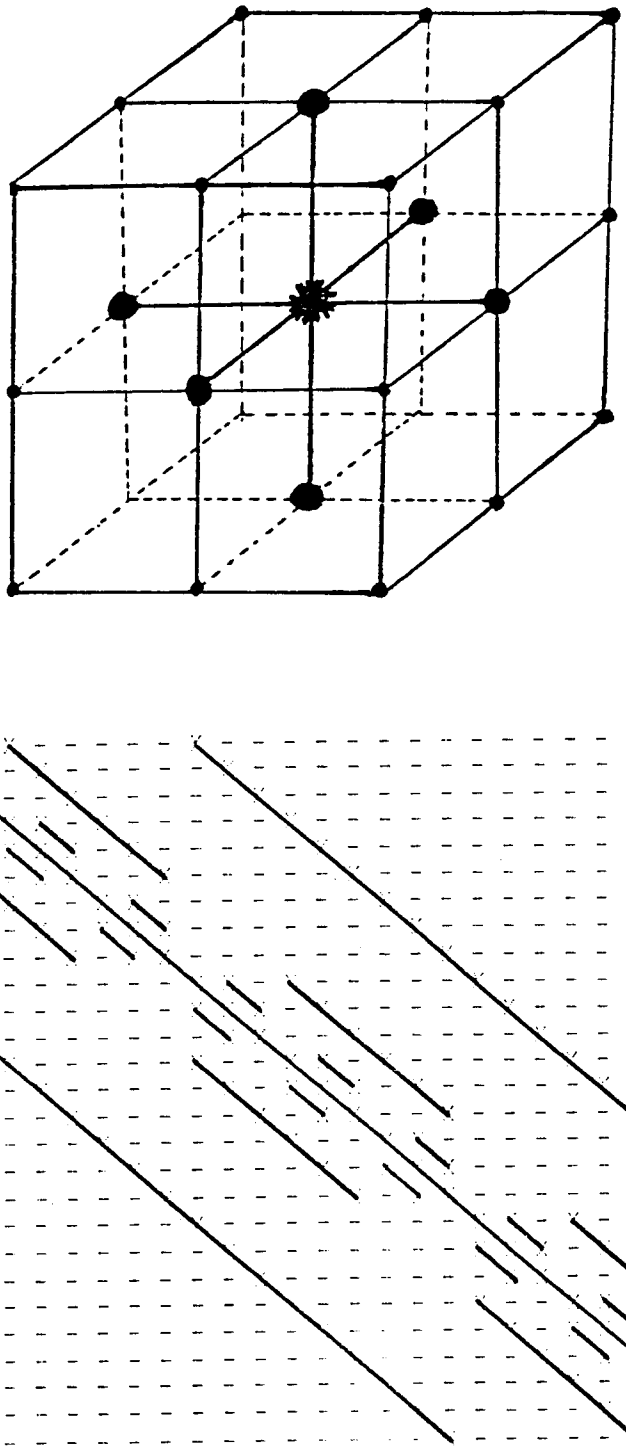

Fig. 2. 7-point centered finite difference scheme and 7-diagonal coefficient matrix.

where each node is connected to six neighbors via one equation, as depicted in Figure 2. As a consequence, the system's matrix A is sparse, seven-diagonal, symmetric, positive-definite, and possesses the so-called 'M-matrix' property (weak diagonal dominance, with all off-diagonal coefficients negative and all diagonal coefficients nonnegative).

The algebraic properties of the finite difference system (8) make it especially well conditioned for the application of 'approximate factorization' methods – or preconditioned iterative methods – such as SIP (Stone, 1968; Weinstein *et al.*, 1969) and ICCG (Meijerink and Van der Vorst, 1977; Kershaw, 1978).* Numerical experiments published in the literature for small problems ($N \simeq 1000$) indicated that SIP and ICCG were more efficient than classical iterative solvers such as ADI and LSOR * (Cooley, 1974; Trescott and Larson, 1977; Kershaw, 1978). Other applications to subsurface flow can be found in Cooley (1974) and McDonald and Harbaugh (1984) for the SIP solver, and Kuiper (1981), Gambolati and Perdon (1984) for the ICCG solver. Related solutions techniques were successfully used in aerodynamics engineering to solve large Navier–Stokes problems with several hundred thousand nodes (Rogallo, 1977; Wray, 1979). For practical reasons, we have chosen to implement the SIP solver, although ICCG may also be considered at later stages of this research.

The properties of SIP were studied by Stone (1968) for the two-dimensional case, and was later extended to three-dimensions by Weinstein *et al.* (1969). The method was applied to three-dimensional groundwater flow problems by Trescott (1975) and McDonald and Harbaugh (1984). The principle of SIP is based on the following formulation of the original finite difference system (8):

$$LU\mathbf{H} = \mathbf{B} + (LU - A)\mathbf{H}, \tag{9}$$

where L and U are lower and upper triangular matrices having the same zero-structure as matrix A. The product LU is an approximation of matrix A, corresponding to a 13 point asymmetric finite difference operator. The system (9) may now be solved by using the Picard-like iteration scheme

$$LU(\mathbf{H}^{m+1} - \mathbf{H}^m) = \mathbf{B} - A\mathbf{H}^m. \tag{10}$$

The computational work involved in finding matrices L, U and in solving directly the above system is proportional to N (around 75 N additions, multiplications, and equivalent divisions) for each iteration. For details on the algorithms, see Weinstein *et al.* (1969) or McDonald and Harbaugh (1984). Our particular implementation of SIP is documented in Ababou *et al.* (1988).

4. Performance of the SIP Solver

The iterative inversion of the finite difference system (Equation (10)) remains a difficult problem due to the large size of the system ($N \approx 10^6$ equations) and the

* SIP: strongly implicit procedure; ICCG: incomplete Choleski-conjugate gradients; ADI: alternate directions implicit; LSOR: line successive over-relaxation.

noisy coefficients. A convenient measure of 'numerical difficulty' is provided by the condition number, ratio of largest to smallest eigenvalue of the coefficient matrix A. For a cubic grid of size $N = n^3$, the condition number is known to behave like n^2 (that is, $N^{2/3}$) in the case $\sigma = 0$. This is a classical result of matrix theory. However, no similar result is available for the random case $\sigma \neq 0$. We conjecture that essentially the same behavior holds true if the mesh size satisfies $\Delta\chi/\lambda \ll \sigma^{-1}$. Thus, for large domain size (L/λ), the condition number of matrix A is presumably proportional to $N^{2/3}$ times an increasing function of σ.

For preconditioned iterative solvers such as SIP, the number of iterations required to reach a given accuracy is known to be proportional to the square root of condition number of the iteration matrix (e.g. LU in Equation (10)). Presumably, the condition of LU is, at worst, on the same order as the condition of the original matrix A. Thus, taking the square root of $N^{2/3}$ leads to order $N^{1/3}$ iterations. This conjecture was recently verified empirically for a wide range of cases (Ababou *et al.*, 1988). Since the computational work per iteration is proportional to N, the total work for a given value of σ should be $N^{4/3}$ (compared to $N^{7/3}$ for a standard band Gauss elimination solver).

Table I shows the performance of the SIP solver for steady saturated flow problems on grids of size 100 000 nodes (actual performance) and one million nodes (predicted performance). The estimated speed-up factor between various machines is displayed at the top of Table I. Most of the numerical experiments involved cubic grids of size $N = 125\,000$ nodes. Accurate solutions were achieved on a Microvax in 7 CPU hours or less, with $\sigma_{\ln K}$ ranging from 1 to 2.3. For larger grids (one million nodes), we expect a CPU time of about 1 h on a vector supercomputer.

The accuracy of the solver was monitored by plotting the logarithm of the residual error norm $\|H^{m+1} - H^m\|$ versus the number of iterations (m). The quadratic norm (root mean square) was further normalized with respect to the head standard deviation (σ_H) which was estimated a-priori from spectral perturbation results.

Table I. CPU time speed-up ratios for various machines compared to Microvax-1 (top), and SIP performance on Microvax and Cray machines (bottom).

IBM PC	Microvax1	Vax 11-782	IBM 370 IBM 3033	Cray 1S scalar	Cray 1S vector
1/5	1	3	10	100	500

Size	Storage (million words)	CPU/ITER (microvax)	Number of iterations	CPU time (microvax)	CPU time (Cray vector)
$N = 10^5$	1.5	4.3 min	100	$\approx$ 7 h	$\approx$ 1 min
$N = 10^6$	15.0	43.0 min	250	$\approx$ 1 week	$\approx$ 0.5 h

Figure 3 shows the decrease of the log-error versus number of iterations for two test problems with different values of the standard deviation of ln K ($\sigma = 1$ and $\sigma = 2.3$). It is clear that convergence is achieved faster for the smaller value of σ. An extremely accurate solution ($\epsilon \simeq 10^{-5}$ to 10^{-6}) is obtained after about 150 iterations for $\sigma = 1$, and 350 iterations for $\sigma = 2.3$. However, the residual error $\|H^{m+1} - H^m\|$ may underestimate the true error $\|H^{m+1} - H^\infty\|$.

In order to improve our estimate of the *true* error, we use the algebraic properties of the solver's iteration matrix. Defining r as the exponential rate of convergence (mean absolute slope of the curves in Figure 3), the true error can be approximated asymptotically as follows (see Remson *et al.*, 1971; Hageman and Young, 1981; Ababou *et al.*, 1988):

$$\|H^{m+1} - H^\infty\| \simeq \|H^{m+1} - H^m\|/(1 - \exp(-r)). \tag{11}$$

From Equation (11) and Figure 3, it appears that the true error must lie below 10^{-4} relative to the head standard deviation. The fact that a constant convergence rate was achieved guarantees the reliability of this estimation. We conclude that numerical 'noise' was negligible compared to the inherent fluctuations of the true solution. This is indeed a very desirable feature given the random nature of the flow field.

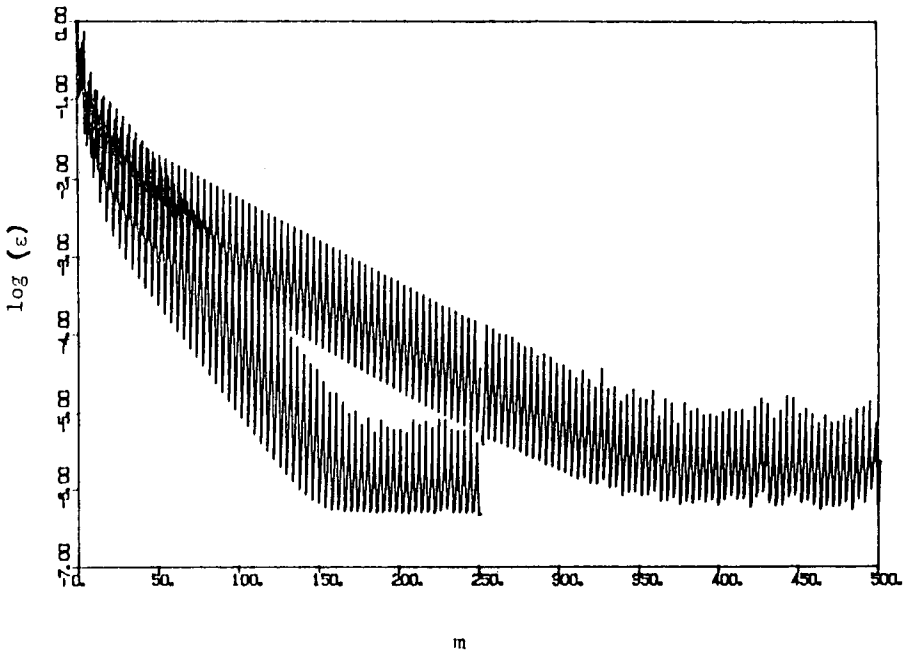

Fig. 3. SIP convergence rate for two test problems: ϵ represents the standardized quadratic norm of residual errors, and m the number of iterations.

5. Analysis of Computed Flow Fields

The two test problems at hand concerned the case of steady saturated flow in a cubic domain, with statistically isotropic conductivities ($\sigma = 1$ and $\sigma = 2.3$). The boundary conditions were fixed heads on two opposite faces, and zero flux on all other boundaries. This, in effect, resulted in imposing a large-scale hydraulic gradient along the mean flow direction ($J_i = 0.004$). The domain size, mesh size and conductivity correlation scale were in the following ratios: $L_i = 25$, $\Delta\chi_i = 0.5$, $\lambda_i = 1$. The finite difference grid size was 125 000 nodes in three dimensions.

The random conductivity field was a single replica of a three-dimensional, statistically isotropic Gauss–Markov process, obtained by the Turning Bands generator (Matheron, 1973; Mantoglou and Wilson, 1982; Tompson *et al.*, 1987). About 100 line processes were used, with a random distribution of lines in space, according to a uniform spherical distribution. The resulting ln K field is Gaussian, with an isotropic exponential covariance function in three-dimensional space. The same replica was used for the two test problems, with $\sigma_{\ln K} = 1$ and 2.3, respectively.

Figure 4 shows low and high conductivity excursion regions (respectively,

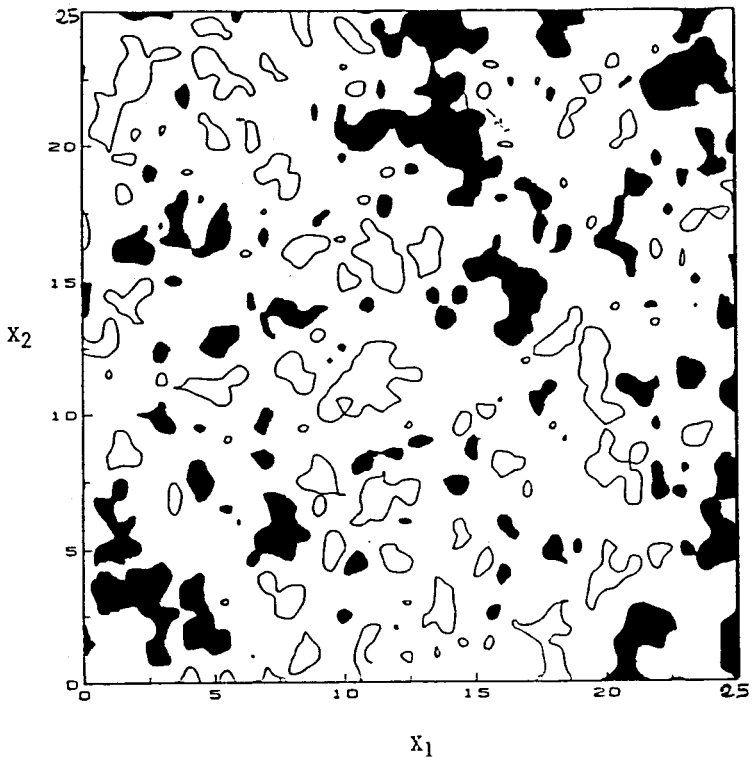

Fig. 4. Excursion regions of the random conductivity field in a two-dimensional slice ($\sigma = 2.3$, $\lambda = 1$). Black and white patches regions where $K \leq 0.1\ K_G$, and $K \geq 10 K_G$, respectively.

black and white) in a two-dimensional slice. For $\sigma = 2.3$, about 40% of the space is occupied by such regions, with the conductivity 10 times below or above the geometric mean. Some of the patches appear to be significantly larger than the correlation length ($\lambda = 1$). As expected, they seem isotropically oriented in space.

Figure 5 displays the contour lines of the computed hydraulic heads in a horizontal slice crossing the center of the cube. The mean hydraulic gradient is parallel to the slice (left to right). Low conductivity contours are also depicted in the background. The head gradient becomes steeper near local minima of conductivity, as could be expected from the Darcy equation. In this example, the conductivity was highly variable ($\sigma = 2.3$).

Figure 6 compares the head contours for $\sigma = 1$ and $\sigma = 2.3$ in the same horizontal slice as Figure 5. The head contours along vertical slices would look essentially the same, due to the statistical isotropy of input conductivities. Overall, the head fields shown in Figures 5 and 6 appear remarkably smooth, despite the noisy input conductivities. This feature is indeed predicted by the spectral perturbation theory.

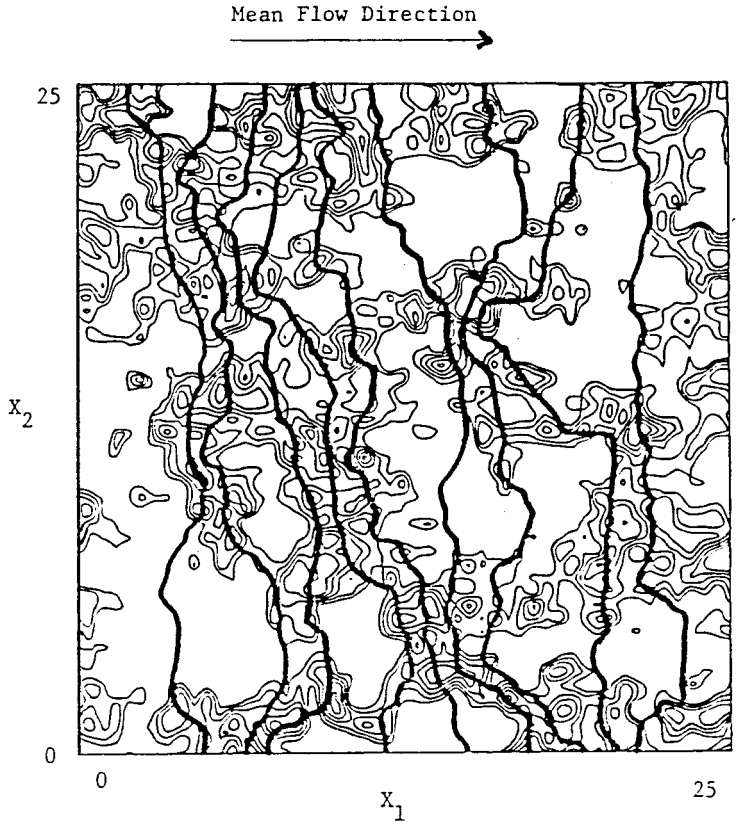

Fig. 5. Hydraulic head contours in a slice parallel to flow for the case $\sigma = 2.3$; low conductivity contours are shown in the background.

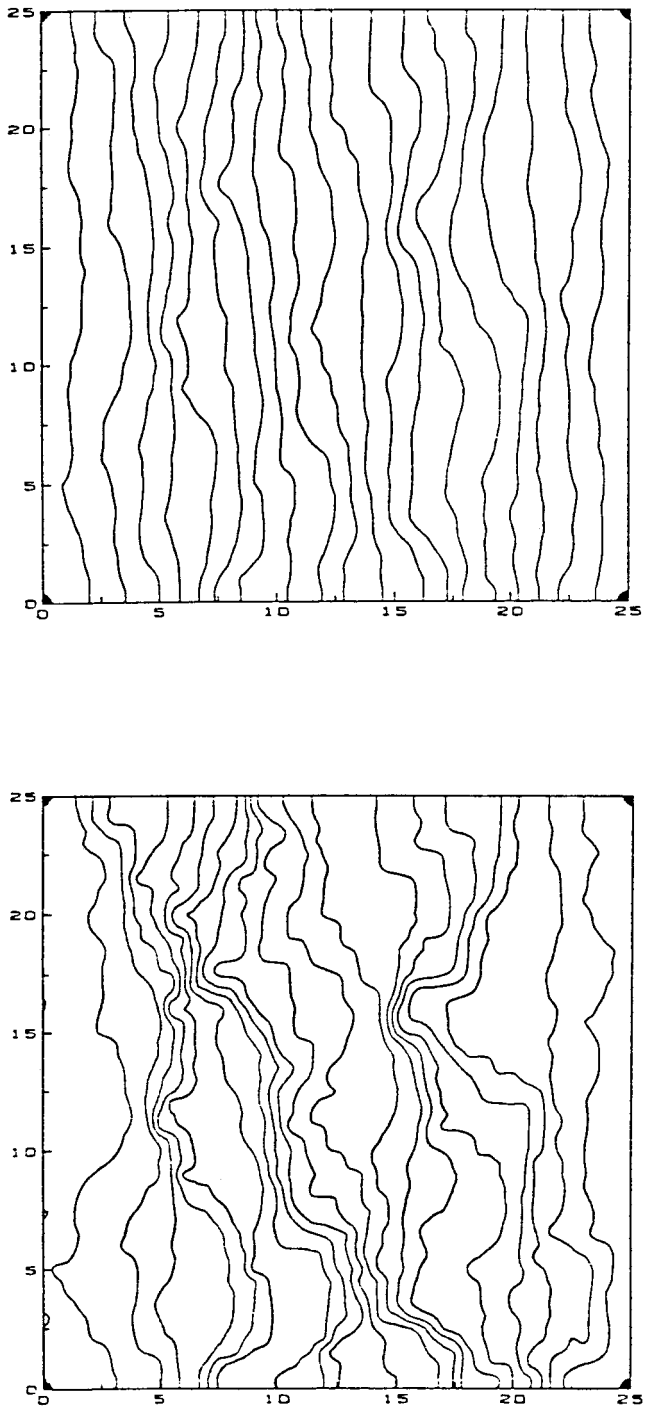

Fig. 6. Comparison of hydraulic head contours for $\sigma = 1$ and $\sigma = 2.3$; the slice is horizontal, parallel to the mean flow.

More precisely, Bakr *et al.* (1978) showed that the head correlation length is about 5λ along the mean flow, and 10λ across flow. Our preliminary calculations using spatial averaging techniques, based on the assumption of stationarity of the detrended head random field, showed that there was at least qualitative agreement for the case $\sigma = 1$. The result was less conclusive in the case $\sigma = 2.3$, probably due to the limited size of the numerical flow domain. In both cases, however, the numerical estimate of head standard deviation (σ_H) matched to within 10% the spectral formula given by Bakr *et al.* (1978)

$$\sigma_H = \frac{1}{\sqrt{3}} \cdot \sigma_{\ln K} \cdot \lambda_{\ln K} \cdot J, \tag{12}$$

as shown in Figure 7.

These results suggest that the predictions of the spectral perturbation theory are quite robust as far as the hydraulic head statistics are concerned. In addition, some preliminary results from spatial moments analyses of numerical velocity fields also seen to be in agreement with theoretical results for moderate variability. The theoretical standard deviations of groundwater velocity and the effective conductivity are given by

$$\sigma_{q_1} = \frac{\sqrt{8}}{\sqrt{15}} \cdot K_G J, \qquad \sigma_{q_2}, \sigma_{q_3} = \frac{1}{\sqrt{15}} \cdot K_G J, \qquad K_e = K_G \cdot \exp\left(\frac{\sigma^2}{6}\right). \tag{13}$$

In particular, the ratio $\sigma_{q_3}/\sigma_{q_1}$ may be thought of as indicating the relative amount of lateral versus longitudinal macroscale dispersion. According to Equation (13), this ratio is constant and equal to $1/\sqrt{8} \approx 0.35$. In the case $\sigma = 1$, about the same value (0.34) was obtained from the numerical velocity fields in the case

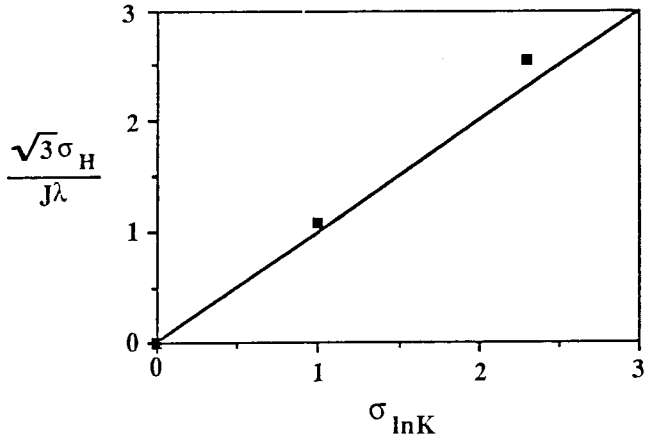

Fig. 7. Comparison of standard deviations of hydraulic head from spectral theory (straight line) and numerical simulations (square dots), versus standard deviation of log-conductivity.

$\sigma = 1$. Also, the normalized effective conductivity K_e/K_G obtained numerically was 1.3, compared to 1.2 from spectral theory.

Finally, the correlation scales of the numerical velocity components (q_i) appeared to be on the order of λ (no greater than 2λ in any direction). This shows that the velocity vector is a 'noisier' random field than the hydraulic head. The velocity spectra obtained from the spectral perturbation theory (Gelhar and Axness, 1983) confirm this view. However, more numerical experiments are needed for a comprehensive characterization of the random velocity field, especially in the case of highly variable media, requiring larger domain size and finer grid resolution.

6. Summary and Discussion

The numerical/single realization approach presented in this paper was aimed at obtaining accurate solutions to the flow equations in highly heterogeneous, random porous media. It is worth nothing that the method does not rely on perturbation approximations, in contrast to presently available analytical results. Indeed, the accuracy of perturbation-based stochastic solutions (Gelhar, 1984; Dagan, 1982) was essentially unknown up to date. On the other hand, other numerical approaches such as Monte Carlo simulation do not specifically take advantage of the statistical information available in one large, single replica. It seems that the present method has the greatest potential for the analysis of large-scale flow behavior whenever some kind of statistical homogeneity can be invoked.

One remarkable feature of the present solution method is the ability to evaluate the solution error along with the solution itself. For the test problems at hand, including a case of highly variable conductivity, the solution error of the iterative finite difference solver was shown to be less than 10^{-4} compared to the standard deviation of the true solution.

On the other hand, it is recognized that the statistical moments of the solution estimated by spatial averaging procedures must be affected by sampling errors. These could, in fact, be routinely evaluated. Our results indicate that the estimation error for σ_H was probably negligible for the given domain size ($L = 25\lambda$).

Another important issue to be considered is the choice of grid resolution. The mesh size should be small enough in order to resolve typical fluctuation scales (λ). In addition, the relative variations of the random conductivity between neighboring grid points should be kept small in some statistical sense. As a rule of thumb based on scaling and statistical arguments, both requirements are embodied in the inequality, $\Delta x/\lambda \leq (1+\sigma)^{-1}$. It seems that this type of requirement has not been emphasized in previous works dealing with numerical approaches such as Monte Carlo simulations.

Encouraging results were obtained, in spite of the limited grid size used in this work (125 000 nodes with a domain size $L = 25\lambda$ and a grid resolution $\Delta x/\lambda =$

0.5). For steady saturated flow with moderate variability, statistical properties such as the head standard deviation, the effective conductivity and the ratio of lateral versus longitudinal velocity standard deviations, all fell within 10% of the predictions of the spectral perturbation theory. Even for a larger variability such as $\sigma_{\ln K} = 2.3$, the theoretical and numerical head variances were in agreement. More work in needed in order to characterize the correlation structure of flow fields (heads and velocities) from numerical single realization simulations.

The spatial structure of the velocity field is particularly important for applications to contaminant transport and large-scale dispersion in the subsurface. However, a comprehensive characterization in terms of variance, correlation structure and probability distribution of the velocity vector is still lacking, except for results obtained by perturbation methods. These implicitly assume that the velocity has a small variance. As σ increases, this assumption probably breaks down, and the distribution of the longitudinal velocity may become positively skewed.

It may be possible to fully characterize the statistical properties of the velocity field in highly variable media if larger numerical grids are used. The numerical experiments in this work required only a few CPU hours on a Microvax machine for grid sizes on the order of 100 000 nodes. We expect that more conclusive results could be obtained on a supercomputer such as a Cray 2, in CPU times on the order of one hour, and with a grid size of one to several million nodes. The standard deviation of the log-conductivity ($\ln K$) could be taken as high as 2.3, a fairly large value according to reported field observations (Gelhar, 1986).

Finally, more complex flow systems ought to be investigated for practical applications to field problems. The single realization approach can be applied to the case of naturally layered aquifers by using statistically anisotropic random functions for the conductivities. Some preliminary results seem to indicate that strongly anisotropic aquifers with moderate thickness behave essentially like slices of two-dimensional flow systems (provided the mean hydraulic gradient is aligned with the statistical bedding). The case of unsaturated flow is also of great interest for waste disposal problems. The vertical mesh size in that case should be taken smaller than both λ and α^{-1}, where α is the slope of the conductivity-pressure relation $\ln K(h)$, and λ the vertical correlation scale. For most soils, it seems, a grid size on the order of 1 000 000 nodes could be sufficient to resolve flow domains of size 10 m in the vertical, and even larger in the horizontal. A nonlinear iterative solver could be used in order to solve stochastic unsaturated flow problems in the framework of the single-realization approach. New results and updates on all the topics mentioned above can be found in the recently published report by Ababou *et al.* (1988).

Acknowledgements

This research was supported in part by the U.S. Nuclear Regulatory Commission (FIN No. B8956) and the National Science Foundation (ECE-8311786). The

material in this paper is essentially that presented in a talk at the International Symposium on the Stochastic Approach to Subsurface Flow which was held in Montvillargenne, France in June 1985 and as such represents an interim report describing ongoing work. More comprehensive simulations have now been completed and the results are described in Ababou *et al.* (1988).

References

Ababou, R., Gelhar, L. W., and McLaughlin, D., 1988, Three-dimensional flow in random porous media, Techn. Report No. 318, Massachusetts Institute of Technology, Ralph Parsons Laboratory, March, 2 volumes.

Bakr, A. A., Gelhar, L. W., Gutjahr, A. L., and MacMillan, R. R., 1978, Stochastic analysis of spatial variability in subsurface flows 1. Comparison of one- and three-dimensional flows, *Water Resour. Res.* **14**(2), 263–271.

Cooley, R. L., 1974, Finite element solutions for the equations of groundwater flow, Techn. Report Seires H-W, 18, University of Nevada, January 84.

Dagan, G., 1982, Stochastic modeling of groundwater flow by conditional and unconditional probabilities: (1) Conditional simulation and the direct problem, *Water Resour. Res.* **18**(4), 813–833.

Freeze, R. A., 1975, Stochastic conceptual analysis of one-dimensional groundwater flow in non-uniform homogeneous media, *Water Resour. Res.* **11**, 725–741.

Gambolati, G. and Perdon, A., 1984, The conjugate gradients in subsurface flow and land subsidence modeling, in J. Bear and M. Y. Corapcioglu (eds), *Fundamentals of Transport Phenomena in Porous Media*, Nijhoff, Dordrecht, pp. 953–984.

Gelhar, L. W., 1984, Stochastic analysis of flow in heterogeneous porous media, in J. Bear and M. Y. Corapcioglu (eds), *Fundamentals of Transport Phenomena in Porous Media*, Nijhoff, Dordrecht, pp. 673–717.

Gelhar, L. W., 1986, Stochastic subsurface hydrology from theory to applications, *Water Resour. Res.* **22**(9), 135–145.

Gelhar, L. W. and Axness, C. L., 1983, Three dimensional stochastic analysis of macrodispersion in aquifers, *Water Resour. Res.* **19**(1), 161–180.

Hageman, L. A. and Young, D. M., 1981, *Applied Iterative Methods*, Academic Press.

Hufschmied, P., 1985, Estimation of three-dimensional statistically anisotropic hydraulic conductivity field by means of single-well pumping tests combined with flowmeter measurements, Paper at the Symposium on the Stochastic Approach to Subsurface Flow, Int. Assoc. Hydraul. Res., Montvillargenne, France, June.

Kershaw, D. S., 1978, The incomplete Choleski-conjugate gradient method for the iterative solution of systems of linear equations, *J. Comput. Phys.* **2–6**, 43–65.

Kuiper, L. K., 1981, A comparison of the incomplete Choleski-conjugate gradient method with the strongly implicit method as applied to the solution of two-dimensional groundwater flow equations, *Water Resour. Res.* **17**(6), 1082–1086.

Lapidus, L. and Pinder, G., 1982, *Numerical Solution of Partial Differential Equations in Science and Engineering*, Wiley-Interscience, New York.

Meijerinck, J. A. and Van Der Vorst, H. A., 1977, An iterative method for linear systems of which the coefficient matrix is a symmetric *M*-matrix, *Math. Comp.* January.

Mantoglou, A. and Wilson, J. L., 1982, The Turning bands method for simulation of random fields using line generation by a spectral method, *Water Resour. Res.* **18**(5), 1379–1394.

Matheron, G., 1973, The intrinsic random functions and their applications, *Adv. Appl. Prob.* **5**, 439–468.

McDonald, M. G. and Harbaugh, A. W., 1984, A modular three-dimensional finite-difference groundwater flow model, USGS Report.

Remson, I., Hornberger, G. M., and Molz, F. J., 1971, *Numerical Methods in Subsurface Hydrology*, Wiley-Interscience, New York.

Rogallo, R. S., 1977, An ILLIAC program for the numerical simulation of the Navier–Stokes equations for a three-dimensional corner, *AIAA J.*, **15**, Nov., 1575–1582.

Stone, H. L., 1968, Iterative solution of implicit approximations of multidimensional partial differential equations, *SIAM J. Numer. Anal.* **5**(3), September.

Tompson, A. F. B., Ababou, R., and Gelhar, L. W., 1987, Application and use of the three-dimensional Turing Bands random field generator (single realization problems), Technical Report No. 313, Massachusetts Institute of Technology, Ralph Parsons Laboratory, March.

Trescott, P. C., 1975, Documentation of finite difference model for simulation of three-dimensional groundwater flow, USGS Open File Report 75-438, September.

Trescott, P. C. and Larson, S. P., 1977, Comparison of iterative methods of solving two-dimensional groundwater flow equations, *Water Resour. Res.* **13**(1).

Weinstein, H. G., Stone, H. L., and Kwan, T. V., 1969, Iterative procedure for solution of systems of parabolic and elliptic equations in three-dimensions, *Industr. Engin. Chem., Fundamentals* **8**(2), 281–287.

Wray, A., 1979, Unpublished results (reported in D. R. Chapman, Computational aerodynamics development and outlook, *AIAA J.* **17**(12)).